Journal of Advanced Ceramics
2015, **4**(2): 135–141
DOI: 10.1007/s40145-015-0145-1

ISSN 2226-4108
CN 10-1154/TQ

Research Article

Influence of variables on the synthesis of $CoFe_2O_4$ pigment by the complex polymerization method

P. N. MEDEIROS[a,*], Y. F. GOMES[a], M. R. D. BOMIO[a], I. M. G. SANTOS[b], M. R. S. SILVA[b], C. A. PASKOCIMAS[a], M. S. LI[c], F. V. MOTTA[a]

[a]*Department of Materials Engineering, Federal University of Rio Grande do Norte, Campus Lagoa Nova, CEP 59078-900-Natal/RN, Brazil*
[b]*Department of Chemistry, Federal University of Paraíba, Cidade Universitária, CEP 58051-900-João Pessoa/PB, Brazi*
[c]*Institute Physics of São Carlos, USP, CEP 13566-590, São Carlos, São Paulo, Brazil*

Received: October 27, 2014; Revised: February 08, 2015; Accepted: February 09, 2015

Abstract: Synthetic inorganic pigments are most widely used in ceramic applications due to their excellent chemical and thermal stability and their lower toxicity to both human and environment as well. In the present work, black ceramic pigment $CoFe_2O_4$ has been synthesized by the complex polymerization method (CPM) with good chemical homogeneity. In order to study the influence of variables on the process of obtaining pigment through CPM, $2^{(5-2)}$ fractional factorial design with resolution III was used. The variables studied in the mathematical modeling were: citric acid/metal concentration, pre-calcination time, calcination temperature, calcination time, and calcination rate. Powder pigments were characterized by X-ray diffraction (XRD), scanning electron microscopy (SEM), and UV–visible (UV–Vis) spectroscopy. Based on the results, the formation of cobalt ferrite phase ($CoFe_2O_4$) with spinel structure was verified. The color of pigments obtained showed dark shades, from black to gray. The model adjusted to the conditions proposed in this study due to the determination coefficient of 99.9% and variance (R^2) showed that all factors are significant at the confidence level of 95%.

Keywords: pigment; complex polymerization method (CPM); fractional factorial design

1 Introduction

Ceramic pigments are powders composed of inorganic oxides consisting of a ceramic matrix of crystalline nature and stable with respect to color when dissolved in glasses or ceramic glazes at high temperatures. The color of each pigment is the result of the addition of chromophore ions (usually transition metals) in an inert matrix (oxide or oxide systems) [1,2].

Usually, a ceramic pigment is a metal transition complex oxide obtained by calcination process with three main characteristics: (a) thermal stability, maintaining its identity when temperature increases; (b) chemical stability, maintaining its identity when fired with glazes or ceramic matrices; and (c) high tinting strength when dispersed and fired with glazes or ceramic matrices. Other characteristics such as high dispensability in vehicles, high refractive index (in order to avoid transparency and to increase its tinting

* Corresponding author.
E-mail: yfeliciano@gmail.com

strength), acid and alkali resistance, and low abrasive strength are also suitable [3].

$CoFe_2O_4$ is typically synthesized using inorganic precursors (primarily nitrate), followed by calcination at high temperature to obtain the spinel structure. A synthesis route frequently investigated in the literature for obtaining $CoFe_2O_4$ at low temperatures is the complex polymerization method (CPM); this study used fractional factorial design to optimize the synthesis process of cobalt aluminate ($CoFe_2O_4$) at operating conditions to determine a means to save time, thus reducing the number of experiments and analyzing the input variables that would influence the process simultaneously [42].

The main coloring methods of ceramics are based on dyes or pigments. In general, a dye or soluble colorant is a colored substance that interacts with the matrix to which it is applied and is usually soluble in the application media called matrix or substrate.

Black pigments are generally produced from the mixture or pure oxides of metals, and the most important oxides in this class of dyes are: cobalt, iron, chromium, and nickel [4,5]. Black pigments are most widely used in the ceramic industry, representing approximately 25% of the total consumption, and are obtained from two main crystalline structures: hematite and spinel [6,7]. Spinel-type pigments are characterized by being stable under the effect of various factors and are widely used in the decoration of ceramic products [8,9].

Cobalt ferrite is a black pigment widely used in the ceramic industry due to its excellent properties such as chemical and thermal stability [10]. Among ferritic materials, $CoFe_2O_4$ has the cubic form of partially inverse spinel [11–13].

Various chemical methods, such as conventional ceramic method [2,14,15], combustion synthesis, co-precipitation [16], sol–gel method [2,17], polymeric precursor [1,18], microwave synthesis [19], and others, have been used to synthesize inorganic pigments. The complex polymerization method (CPM) based on the Pechini method offers the possibility of preparing complexes of good homogeneity at molecular scale and a good stoichiometric control. The temperatures required are lower than in conventional methods, as in reactions between materials in the solid state or decompositions [20–24]. Many variables can influence the synthesis of oxides by CPM [25–27]. Therefore, an experimental design should be used to investigate the factors that most influence the results.

The experimental design consists of a set of tests established with statistical criteria aimed at determining the influence of variables on the results of a given system or process. The benefits are the reduced number of trials without compromising the quality of information, simultaneous study of several variables, and representation of the process studied by mathematical expressions [28–31].

In this study, a $2^{(5-2)}$ fractional factorial design was used to evaluate the influence of variables on the synthesis of $CoFe_2O_4$ by CPM. It optimized the process of cobalt ferrite ($CoFe_2O_4$) synthesis at operating conditions to determine a means to save time, thus reducing the number of experiments and analyzing the input variables that would influence the process simultaneously.

2 Experimental

2. 1 Materials and reagents

Cobalt nitrate ($CoN_2O_6{\cdot}6H_2O$, Aldrich, 98%), iron nitrate ($Fe(NO_3)_3{\cdot}9H_2O$, Synth, 99%), citric acid ($C_6H_8O_7{\cdot}H_2O$, Synth, 99.5%), and ethylene glycol ($C_2H_6O_2$, Synth, 99%) were used to prepare the cobalt ferrite precursor resins ($CoFe_2O_4$).

2. 2 Experimental design

The fractional factorial design increases the amount of information obtained and reduces the number of experiments with the aim of studying the influence of variables on the synthesis of cobalt ferrite through CPM; a series of experiments were carried out according to a statistical experimental design using the STATISTIC Software 7.0 [32].

To build the design matrix of experiments, five factors were chosen, each with two levels, resulting in 32 combinations. However, a $2^{(5-2)}$ fractional factorial design with resolution III was used. When using a $2^{(5-2)}$ experiment with eight combinations (only one fourth of the entire experiment), the number of experiments, the time spent on the experiments, and the consumption of reagents were reduced. The five factors were: citric acid/metal concentration, pre-calcination time, calcination temperature, calcination time, and calcination rate, assessed on two levels (–1 and +1) and three replicates at the center point (0), totaling 11 experiments. In response, the mean reflectance percentage in the visible range (400–

700 nm) for each sample synthesized was used. The syntheses were carried out according to the scheme shown in Table 1.

The $2^{(5-2)}=2^3$ fractional factorial approach reduced the number of experiments to 11, including eight factorial and three central points.

The values of wavelengths (Y) related to higher peak absorbance of pigments obtained by UV–visible (UV–Vis) spectroscopy analysis are the response variables. Based on this analysis [42], the general second-order or quadratic equation may be generated, as represented in Eq. (1):

$$Y=\beta_0+\sum_{j=1}^{k}\beta_j x_j+\sum\sum_{i<j}\beta_{ij}x_i x_j+\sum_{j=1}^{k}\beta_{jj}x_j^2+\varepsilon \quad (1)$$

where Y is the expected response wavelength; x_i is the encoded or non-encoded value of factors (citric acid/metal concentration, pre-calcination time, calcination temperature, calcination time, and calcination rate); β_0 is a constant; i is the leading coefficient for each variable; and ij is the effect of the interaction of coefficients [42].

The values of polynomial coefficients and the response surface of the second-order model were obtained using the STATISTICA Software 7.0, and the model was validated for the processing conditions used in this study.

2. 3 Cobalt ferrite synthesis

The materials used to obtain cobalt ferrite were citric acid, iron nitrate, cobalt nitrate, and ethylene glycol. Initially, citric acid was dissolved in distilled water under stirring and heating at about 70 ℃. After dissolution, iron nitrate was added and then cobalt nitrate, with citric acid/metal ratio according to the experimental design. Then, ethylene glycol was added at a weight ratio of 60∶40 in relation to citric acid. The heating temperature was kept at about 75 ℃ for the polymerization of the esterification reaction. The reduction of the solution volume was expected to occur for the removal of excess solvent resulting in a viscous material, the polymeric resin. This gel was submitted to pre-calcination in a muffle furnace at 350 ℃ by the time determined in the statistical planning. Subsequently, the material was deagglomerated and approximately 2 g was removed for thermal analysis. The rest of powders were calcined at 700 ℃, 800 ℃, and 900 ℃ according to the experimental design.

Pigments were characterized by X-ray diffraction (XRD) on a Shimadzu XRD-7000 diffractometer using Cu Kα radiation. The morphology of pigment particles after calcination was observed in a scanning electron microscope (SEM) from Hitachi High Technologies. UV–Vis spectroscopy analyses were performed on a Shimadzu UV–visible brand, with accessory reflectance UV-2550, with wavelength in the region between 190 and 900 nm

Table 1 $2^{(5-2)}$ fractional factorial design with three replicates at the center point

Experiment	Citric acid/metal concentration	Pre-calcination time (h)	Calcination temperature (℃)	Calcination time (h)	Calcination rate (℃/min)
1	2:1 (–1)	1 (–1)	700 (–1)	6 (1)	11 (1)
2	4:1 (1)	1 (–1)	700 (–1)	2 (–1)	5 (–1)
3	2:1 (–1)	3 (1)	700 (–1)	2 (–1)	11 (1)
4	4:1 (1)	3 (1)	700 (–1)	6 (1)	5 (–1)
5	2:1 (–1)	1 (–1)	900 (1)	6 (1)	5 (–1)
6	4:1 (1)	1 (–1)	900 (1)	2 (–1)	11 (1)
7	2:1 (–1)	3 (1)	900 (1)	2 (–1)	5 (–1)
8	4:1 (1)	3 (1)	900 (1)	6 (1)	11 (1)
9	3:1 (0)	2 (0)	800 (0)	4 (0)	8 (0)
10	3:1 (0)	2 (0)	800 (0)	4 (0)	8 (0)
11	3:1 (0)	2 (0)	800 (0)	4 (0)	8 (0)

3 Results and discussion

3. 1 Characterization of $CoFe_2O_4$ particles

Reflectance measurements were used to characterize the optical behavior of the pigments obtained in the visible region. Typical reflectance curves are illustrated in Fig. 1. The results obtained in response to the experimental design are shown in Table 2. The results for all $CoFe_2O_4$ powders synthesized show absorption band in the entire visible wavelength range, which is typical of low-reflectance systems, indicating the formation of dark-colored pigments [6]. The charge transfer between Co–O and Fe–O along with d–d electronic transitions of Co^{2+} and Fe^{3+} in multiple

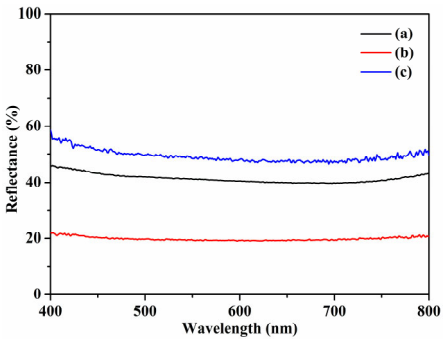

Fig. 1 Reflectance spectra of $CoFe_2O_4$ particles obtained by experiments (a) 4, (b) 7, and (c) 9.

Table 2 Results of the reflectance percentage of $CoFe_2O_4$ particles

Experiment	Reflectance (%)
1	25.60
2	14.60
3	28.12
4	41.65
5	37.09
6	48.77
7	19.78
8	46.06
9	49.46
10	49.35
11	49.68

coordination ensures complete absorption throughout the visible spectrum [12].

According to the literature, the reflectance curve of theoretical black color would present 0% reflectance at all wavelengths. However, in practice, it is observed that a pigment with the best possible black color shows reflectance values close to 0% in the visible wavelength range [33,34].

In Fig. 2, photomicrographs of cobalt ferrite pigments show black color by using the obtained statistical design values of factors (citric acid/metal concentration, pre-calcination time, calcination temperature, calcination time, and calcination rate) and the route from polymeric precursors.

All $CoFe_2O_4$ samples were characterized by XRD. Figure 3 shows the XRD patterns obtained from experiments 4, 7, and 9. According to the statistical design (Table 1), in general, in all powders, the major phase of the $CoFe_2O_4$ spinel structure was identified

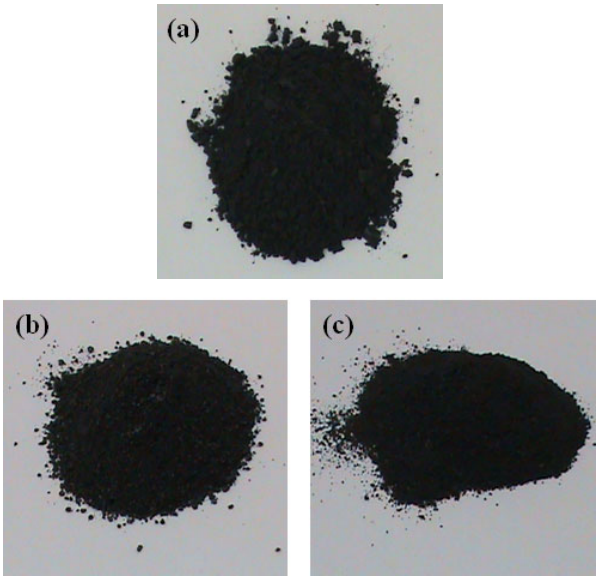

Fig. 2 Photomicrographs of cobalt ferrite pigments showing black color by using the obtained statistical design experiments (a) 4, (b) 7, and (c) 9.

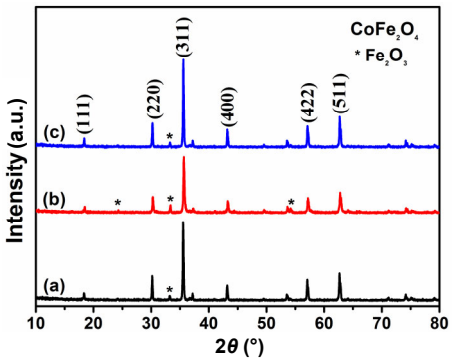

Fig. 3 XRD patterns of $CoFe_2O_4$ particles obtained by experiments (a) 4, (b) 7, and (c) 9.

according to the JCPDS 22-1086 form [35–39].

In micrographs obtained for $CoFe_2O_4$ samples, a strong agglomeration is evidenced in all compounds, which is attributed to both the synthesis method used and the magnetic characteristic of the material, which is due to the attraction between particles tending to form clusters [40]. Another factor that can lead to the formation of partially sintered agglomerates is additional heating due to the combustion of the organic material during calcination [41]. Figure 4 shows the morphology of particles obtained from experiments 4, 7, and 9.

3.2 Experimental design

The experimental design was analyzed using the STATISTICA software and analysis of variance (ANOVA), which evaluate whether the effect and interaction between the factors investigated are of significance with regard to the experimental error. The significance of the main factors and their interactions were evaluated by the F-test with 95% confidence

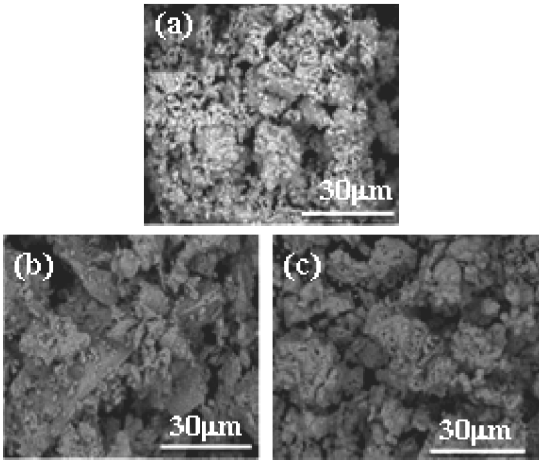

Fig. 4 SEM micrographs of $CoFe_2O_4$ particles obtained by experiments (a) 4, (b) 7, and (c) 9.

level (Table 3) [42].

The results of the ANOVA analysis are presented in Table 3, showing that all the effects and interactions between the factors are significant ($P < 0.05$).

The estimated effects and coefficients are listed in Table 4. The experimental error and the main factors and their interactions were evaluated by the F-test with 95% confidence level as reported by Montgomery [42] and Mason *et al*. [32]. Table 4 shows the main effects and interactions of independent variables and as response, the reflectance percentage for a linear model, considering the interactions between variables with 95% confidence level. Data were obtained considering the pure error.

Table 3 Analysis of variance (ANOVA) for the suggested model

Source	DF	SS	MS	*F*	*P*
(1) Citric acid/metal concentration	1	204.971	204.970	7619.44	0.000131
(2) Pre-calcination time (h)	1	11.386	11.386	423.26	0.002354
(3) Calcination temperature (℃)	1	217.799	217.799	8096.33	0.000123
(4) Calcination time (h)	1	191.375	191.375	7114.05	0.000141
(5) Calcination rate (℃/min)	1	156.840	156.840	5830.26	0.000171
(3)×(4)	1	12.301	12.301	457.26	0.002180
(4)×(5)	1	307.322	307.322	11424.17	0.000088
(1)×(3)×(5)	1	614.789	614.789	22853.75	0.000044
Pure error	2	0.054	0.0269		
Total	10	1716.836			

DF: degree of freedom; SS: sum of square; MS: mean square; and *F*: F-test.

Table 4 Estimated effects of the experimental design

	Effect	Pure error	t(2)	*P*	Confidence level 95%
Mean/ interaction	49.4960	0.094694	522.693	0.000004	(49.0886; 49.9034)
(1) Citric acid/metal concentration	10.1235	0.115976	87.289	0.000131	(9.6245; 10.6225)
(2) Pre-calcination time (h)	2.3860	0.115976	20.576	0.002354	(1.8870; 2.8850)
(3) Calcination temperature (℃)	10.4355	0.115976	89.980	0.000123	(9.9365; 10.9345)
(4) Calcination time (h)	9.7820	0.115976	84.345	0.000141	(9.2830; 10.2810)
(5) Calcination rate (℃/min)	8.8555	0.115976	76.356	0.000171	(8.3565; 9.3545)
(3)×(4)	–2.4800	0.115976	–21.384	0.002180	(–2.9790; –1.9810)
(4)×(5)	–12.396	0.115976	–106.884	0.000088	(–12.8950; –11.8970)
(1)×(3)×(5)	–33.5725	0.222078	–151.175	0.000044	(–34.5280; –32.6170)

$R^2 = 0.99997$; adjustment: 0.99984; MS pure error = 0.026901.

As illustrated in the Pareto diagram (Fig. 5), effects are statistically significant on the response variables. It is observed that the determination coefficient (R^2) is approximately 99.99%, indicating that a linear model is able to represent the relationship between effects and response.

In the Pareto chart, the five input variables with values greater than 87.28939 ($P = 0.05$) at the right of the line are significant; the calcination temperature has greater statistical significance compared to the other factors studied. The negative value of –151.175 indicates higher values of the reflectance range to the lower level with respect to the calcination time. The calcination rate shows positive numeric value of 76.35612, indicating an increase in the reflectance value when the citric acid/metal concentration reaches its maximum level (Fig. 5).

In Fig. 6, the values predicted by the model are represented by the straight line, while observed values are represented by points. Predicted values versus observed values using the model equation were obtained from data of the response surface of UV–Vis absorbance. Effects with less than 95% significance according to the F-test used in this study are not reported. Observed values are close to predicted values, demonstrating that the model is adequate (Fig. 6).

Based on the significant effects, the following model (Eq. (2)) is proposed:

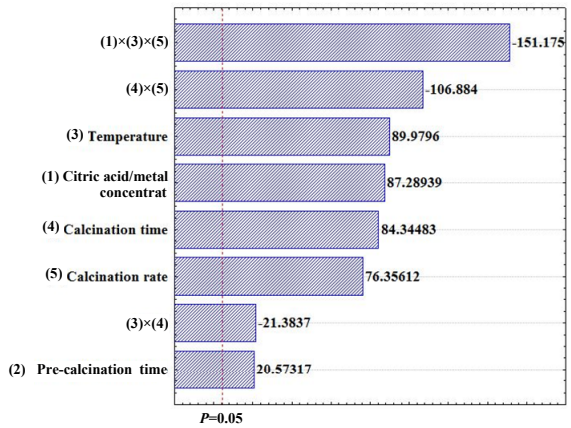

Fig. 5 Pareto diagram of the $2^{(5-2)}$ fractional factorial design showing the influence of the factors studied.

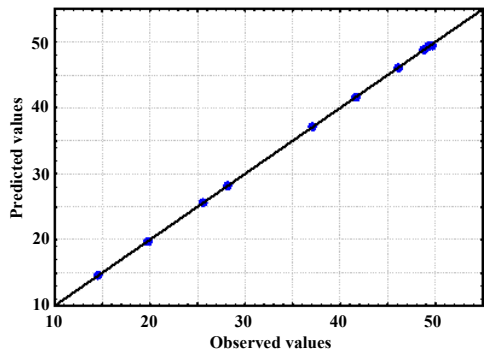

Fig. 6 Values predicted by the model versus observed values, according to the reflectance values.

$$Y = 49.496 + (4.891 \times \text{Calcination time}) + (4.42775 \times \text{Calcination rate}) - (1.241 \times \text{Calcination time}) - (6.198 \times \text{Calcination time} \times \text{Calcination rate}) - (16.78625 \times \text{Calcination rate}) + 11.4725 \quad (2)$$

The wavelength model equation is expressed to the following interval (–1, 0, +1), or variables citric acid/metal concentration, pre-calcination time, calcination temperature, calcination time, and calcination rate.

Equation (2) was used to predict the wavelength, in which the model function is valid for the defined interval, i.e., for variables citric acid/metal concentration, pre-calcination time, calcination temperature, calcination time, and calcination rate. In the valid range from –1 to +1 for the experimental conditions used in this study, the determination coefficient of the proposed mathematical model can explain about 99.9% of the variance (R^2) [32,42].

The results of experiments show that all variables influence in synthesis of cobalt ferrite by CPM; however, the interaction between citric acid/metal concentration, calcination temperature, and calcination rate is more significant.

4 Conclusions

The results obtained in this study indicated that the CPM was favorable for the synthesis of $CoFe_2O_4$ pigment with spinel structure. XRD showed that the $CoFe_2O_4$ phase was obtained for all samples, some of which showed Fe_2O_3 and Co_3O_4 as secondary phases. The spectra in the UV–Vis region indicated that the synthesized pigment showed darker shades, with color predominantly from black to gray.

According to the $2^{(5-2)}$ fractional factorial design, it was observed that all main effects were significant, as well as the interactions between effects, at confidence level of 95%. The linear model showed optimal adjustment with $R^2 = 99.99\%$, being also statistically significant. The design of experiments used showed that all variables studied influence the production of cobalt ferrite pigment by CPM.

Acknowledgements

The authors thank the financial support of the Brazilian research financing institutions: RECAM (Rede de Catalisadores Ambientais), CNPq, and CAPES.

References

[1] Cunha JD, Melo DMA, Martinelli AE, *et al*. Ceramic pigment obtained by polymeric precursors. *Dyes Pigments* 2005, **65**: 11–14.

[2] Gorodylova N, Kosinová V, Dohnalová Ž, *et al.* New purple-blue ceramic pigments based on $CoZr_4(PO_4)_6$. *Dyes Pigments* 2013, **98**: 393–404.

[3] Monrós G. *Pigment*, *Ceramic*, *Encyclopedia of Color Science and Technology*. Springer, 2014.

[4] Escardino A, Mestre S, Barba A, *et al.* Kinetic study of black Fe_2O_3–Cr_2O_3 pigment synthesis: I, influence of synthesis time and temperature. *J Am Ceram Soc* 2003, **86**: 945–950.

[5] Zaichuk AV, Belyi YI. Black ceramic pigments based on open-hearth slag. *Glass Ceram*+ 2012, **69**: 99–103.

[6] Costa G, Della VP, Ribeiro MJ, *et al.* Synthesis of black ceramic pigments from secondary raw materials. *Dyes Pigments* 2008, **77**: 137–144.

[7] Hajjaji W, Seabra MP, Labrincha JA. Evaluation of metal-ions containing sludges in the preparation of black inorganic pigments. *J Hazard Mater* 2011, **185**: 619–625.

[8] Maslennikova GN. Pigments of the spinel type. *Glass Ceram*+ 2001, **58**: 216–220.

[9] Mestre S, Palacios MD, Agut P. Solution combustion synthesis of $(Co,Fe)Cr_2O_4$ pigments. *J Eur Ceram Soc* 2012, **32**: 1995–1999.

[10] Yüngevis H, Ozel E. Effect of the milling process on the properties of $CoFe_2O_4$ pigment. *Ceram Int* 2013, **39**: 5503–5511.

[11] Liu X-M, Fu S-Y, Xiao H-M, *et al.* Synthesis of nanocrystalline spinel $CoFe_2O_4$ via a polymer-pyrolysis

route. *Physica B* 2005, **370**: 14–21.
[12] Cavalcante PMT, Dondi M, Guarini G, *et al*. Colour performance of ceramic nano-pigments. *Dyes Pigments* 2009, **80**: 226–232.
[13] Jia Z, Ren D, Zhu R. Synthesis, characterization and magnetic properties of $CoFe_2O_4$ nanorods. *Mater Lett* 2012, **66**: 128–131.
[14] Costa G, Ribeiro MJ, Hajjaji W, *et al.* Ni-doped hibonite ($CaAl_{12}O_{19}$): A new turquoise blue ceramic pigment. *J Eur Ceram Soc* 2009, **29**: 2671–2678.
[15] Gargori C, Cerro S, Galindo R, *et al.* New vanadium doped calcium titanate ceramic pigment. *Ceram Int* 2011, **37**: 3665–3670.
[16] Llusar M, Zielinska A, Tena MA, *et al.* Blue-violet ceramic pigments based on Co and Mg $Co_{2-x}Mg_xP_2O_7$ diphosphates. *J Eur Ceram Soc* 2010, **30**: 1887–1896.
[17] Ricceri R, Ardizzone S, Baldi G, *et al.* Ceramic pigments obtained by sol–gel techniques and by mechanochemical insertion of color centers in Al_2O_3 host matrix. *J Eur Ceram Soc* 2002, **22**: 629–637.
[18] Melo D, Vieira FTG, Costa TCC, *et al.* Lanthanum cobaltite black pigments with perovskite structure. *Dyes Pigments* 2013, **98**: 459–463.
[19] Blosi M, Albonetti S, Gatti F, *et al.* Au–Ag nanoparticles as red pigment in ceramic inks for digital decoration. *Dyes Pigments* 2012, **94**: 355–362.
[20] Kakihana M. Invited review "sol–gel" preparation of high temperature superconducting oxides. *J Sol–Gel Sci Technol* 1996, **6**: 7–55.
[21] Bernardi MIB, De Vicente FS, Li MS, *et al*. Colored films produced by electron beam deposition from nanometric TiO_2 and Al_2O_3 pigment powders obtained by modified polymeric precursor method. *Dyes Pigments* 2007, **75**: 693–700.
[22] Cho W-S, Kakihana M. Crystallization of ceramic pigment $CoAl_2O_4$ nanocrystals from Co–Al metal organic precursor. *J Alloys Compd* 1999, **287**: 87–90.
[23] Razpotnik T, Maček J. Synthesis of nickel oxide/zirconia powders via a modified Pechini method. *J Eur Ceram Soc* 2007, **27**: 1405–1410.
[24] Mariappan CR, Galven C, Crosnier-Lopez M-P, *et al.* Synthesis of nanostructured $LiTi_2(PO_4)_3$ powder by a Pechini-type polymerizable complex method. *J Solid State Chem* 2006, **179**: 450–456.
[25] Vieira FTG, Melo DS, de Lima SJG, *et al.* The influence of temperature on the color of TiO_2:Cr pigments. *Mater Res Bull* 2009, **44**: 1086–1092.
[26] Chai Y-L, Chang Y-S, Chen G-J, *et al.* The effects of heat-treatment on the structure evolution and crystallinity of $ZnTiO_3$ nano-crystals prepared by Pechini process. *Mater Res Bull* 2008, **43**: 1066–1073.
[27] Mohammadia MR, Fray DJ. Low temperature nanostructured zinc titanate by an aqueous particulate sol–gel route: Optimisation of heat treatment condition based on Zn:Ti molar ratio. *J Eur Ceram Soc* 2010, **30**: 947–961.
[28] Box GEP, Hunter WG, Hunter JS. *Statistic for Experiments*: *Design, Innovation, and Discovery*, 2nd edn. New York: Wiley, 2005.
[29] Rautio J, Perämäki P, Honkamo J, *et al.* Effect of synthesis method variables on particle size in the preparation of homogeneous doped nano ZnO material. *Microchem J* 2009, **91**: 272–276.
[30] Rosario AV, Pereira EC. Comparison of the electrochemical behavior of CeO_2–SnO_2 and CeO_2–TiO_2 electrodes produced by the Pechini method. *Thin Solid Films* 2002, **410**: 1–7.
[31] Maran JP, Manikandan S. Response surface modeling and optimization of process parameters for aqueous extraction of pigments from prickly pear (*Opuntia ficus-indica*) fruit. *Dyes Pigments* 2012, **95**: 465–472.
[32] Mason RL, Gunst RF, Hess JL. *Statistical Design and Analysis of Experiments*: *With Aplications to Engineering and Science*, 2nd edn. New Jersey: John Wiley & Sons, 2003.
[33] Sánchez MYH, Baena OJR. Síntesis y caracterización colorimétrica de un pigmento negro tipo espinela. CONAMET/SAM-2008.
[34] Shen L, Qiao Y, Guo Y, *et al*. Preparation of nanometer-sized black iron oxide pigment by recycling of blast furnace flue dust. *J Hazard Mater* 2010, **177**: 495–500.
[35] Sajjia M, Oubaha M, Prescott T, *et al*. Development of cobalt ferrite powder preparation employing the sol–gel technique and its structural characterization. *J Alloys Compd* 2010, **506**: 400–406.
[36] Verma KC, Singh VP, Ram M, *et al*. Structural, microstructural and magnetic properties of $NiFe_2O_4$, $CoFe_2O_4$ and $MnFe_2O_4$ nanoferrite thin films. *J Magn Magn Mater* 2011, **323**: 3271–3275.
[37] Airimioaei M, Ciomaga CE, Apostolescu N, *et al*. Synthesis and functional properties of the $Ni_{1-x}Mn_xFe_2O_4$ ferrites. *J Alloys Compd* 2011, **509**: 8065–8072.
[38] Lavela P, Tirado JL. $CoFe_2O_4$ and $NiFe_2O_4$ synthesized by sol–gel procedures for their use as anode materials for Li ion batteries. *J Power Sources* 2007, **172**: 379–387.
[39] Simões AZ, Riccardi CS, Dos Santos ML, *et al*. Effect of annealing atmosphere on phase formation and electrical characteristics of bismuth ferrite thin films. *Mater Res Bull* 2009, **44**: 1747–1752.
[40] Gimenes R, Baldissera MR, da Silva MRA, *et al*. Structural and magnetic characterization of $Mn_xZn_{1-x}Fe_2O_4$ ($x = 0.2$; 0.35; 0.65; 0.8; 1.0) ferrites obtained by the citrate precursor method. *Ceram Int* 2012, **38**: 741–746.
[41] Popa M, Calderon-Moreno JM. Lanthanum cobaltite nanoparticles using the polymeric precursor method. *J Eur Ceram Soc* 2009, **29**: 2281–2287.
[42] Montgomery DC. *Design and Analysis of Experiments*, 5th edn. New York: Wiley, 2001.